Results in Engineering 32 (2026) 111662

Contents lists available at ScienceDirect

Results in Engineering

journal homepage: www.sciencedirect.com/journal/results-in-engineering

Research paper

Investigating the effect of variable electric-field amplitude and frequency on the interaction of water/silver nanofluid with the SARS-CoV-2 main protease: a molecular dynamics study

Ali Alkhafaji [a], Ahmed Mohammed Attyah Zheoat [b], Mohammed R. Hashim Al-Dahhan [c], Narinderjit Singh Sawaran Singh [d], Banaz Shahab Haji [e], Hakim AL Garalleh [f], Zuhair Jastaneyah [l], Soheil Salahshour [g,h,i,j,*], Mahmut Taner [k,*]

[a] Advanced Technical College, University of Warith Al-Anbiyaa, Karbala, Iraq
[b] Department of Pharmacology and Toxicology, College of Pharmacy, University of Manara, Amarah, Maysan, Iraq
[c] Department of Computer Sciences, College of Science, University of Al Maarif, Al Anbar, 31001, Iraq
[d] Faculty of Data Science and Information Technology, INTI International University, Persiaran Perdana BBN, Putra Nilai, Nilai, 71800, Malaysia
[e] Medical Radiology Imaging Department, College of Health Sciences, Lebanese French University (LFU), Kurdistan Region, Erbil, Iraq
[f] Department of Mathematical Science, College of Engineering, University of Business and Technology, Jeddah, 21361, Saudi Arabia
[g] Faculty of Engineering and Natural Sciences, Istanbul Okan University, Istanbul, Turkey
[h] Faculty of Engineering and Natural Sciences, Bahcesehir University, Istanbul, Turkey
[i] Research Center of Applied Mathematics, Khazar University, Baku, Azerbaijan
[j] Faculty of Science and Letters, Piri Reis University, Tuzla, Istanbul, Turkey
[k] Faculty of Engineering and Architecture, Istanbul Gelisim University, Istanbul, Türkiye
[l] Department of Mechanical Engineering, College of Engineering, University of Business and Technooogy, Jeddah 21361, Saudi Arabia

ARTICLE INFO

Keywords:
External electric field
Nanofluid
SARS-CoV-2 Virus
Molecular dynamics simulation
Infectious Disease

ABSTRACT

This study investigated the effect of external electric fields on the interactions between water/silver nanofluids and the SARS-CoV-2 main protease using molecular dynamics simulations. The primary objective was to evaluate how variations in electric-field strength and frequency influenced the mobility of nanofluid particles and the structural stability of viral protease at the atomic scale. Following system equilibration at physiological temperature, electric fields with amplitudes ranging from 0.1 to 0.5 V/Å and frequency parameters ranging from 0.01 to 0.04 fs^{-1} were applied. The results demonstrate that increasing the electric-field amplitude significantly enhanced nanofluid mobility within the protease environment, as reflected by an increase in the diffusion coefficient from 75.19 to 235.25 nm^2/ns and a change in the interaction energy from −312.32 to −122.80 kcal/mol. These changes indicated stronger field-induced perturbations and modified protein–nanofluid interactions. In contrast, increasing the electric-field frequency at a fixed amplitude of 0.4 V/Å decreased the diffusion coefficient from 141.19 to 68.94 nm^2/ns and changed the interaction energy from −83.14 to −259.35 kcal/mol, indicating reduced atomic mobility and enhanced interaction stability. Overall, the findings reveal that higher electric-field amplitudes intensified nanofluid transport and promoted structural perturbations of SARS-CoV-2 main protease, whereas higher frequencies partially suppressed these effects. These results provide atomistic insight into the coupled influence of electric fields and nanofluids on viral protein behavior and may contribute to the development of electrically assisted nanomaterial-based antiviral technologies.

1. Introduction

Coronaviruses belong to the Coronaviridae family and can infect the respiratory tract of humans and animals. Their clinical effects range from mild respiratory symptoms to severe diseases, such as MERS, SARS, and COVID-19 [1–5]. The global impact of SARS-CoV-2 has increased interest in physical, chemical, and nanomaterial-based strategies to reduce viral stability, disrupt viral proteins, or limit viral transmission. Previous studies mainly focused on viral survival on surfaces, environmental transmission, climatic effects, airborne particles, and the general

* Corresponding authors.
E-mail addresses: soheil.salahshour1361@gmail.com (S. Salahshour), mtaner@gelisim.edu.tr (M. Taner).

https://doi.org/10.1016/j.rineng.2026.111662
Received 13 May 2026; Received in revised form 11 June 2026; Accepted 21 June 2026
Available online 21 June 2026

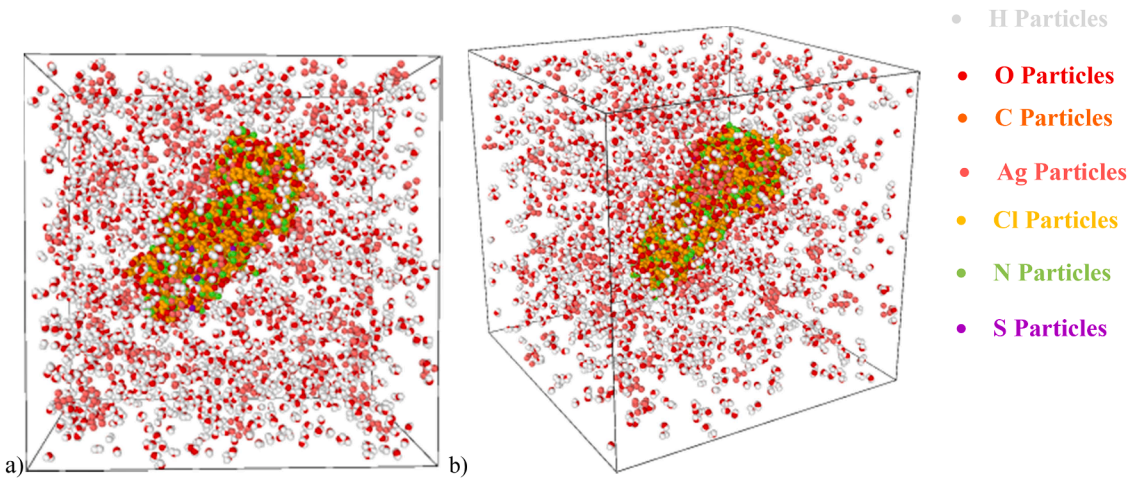

Fig. 1. Simulation system used in the molecular dynamics study: (a) side view and (b) perspective view of the simulation box containing the SARS-CoV-2 main protease, water molecules, and silver nanoparticles.

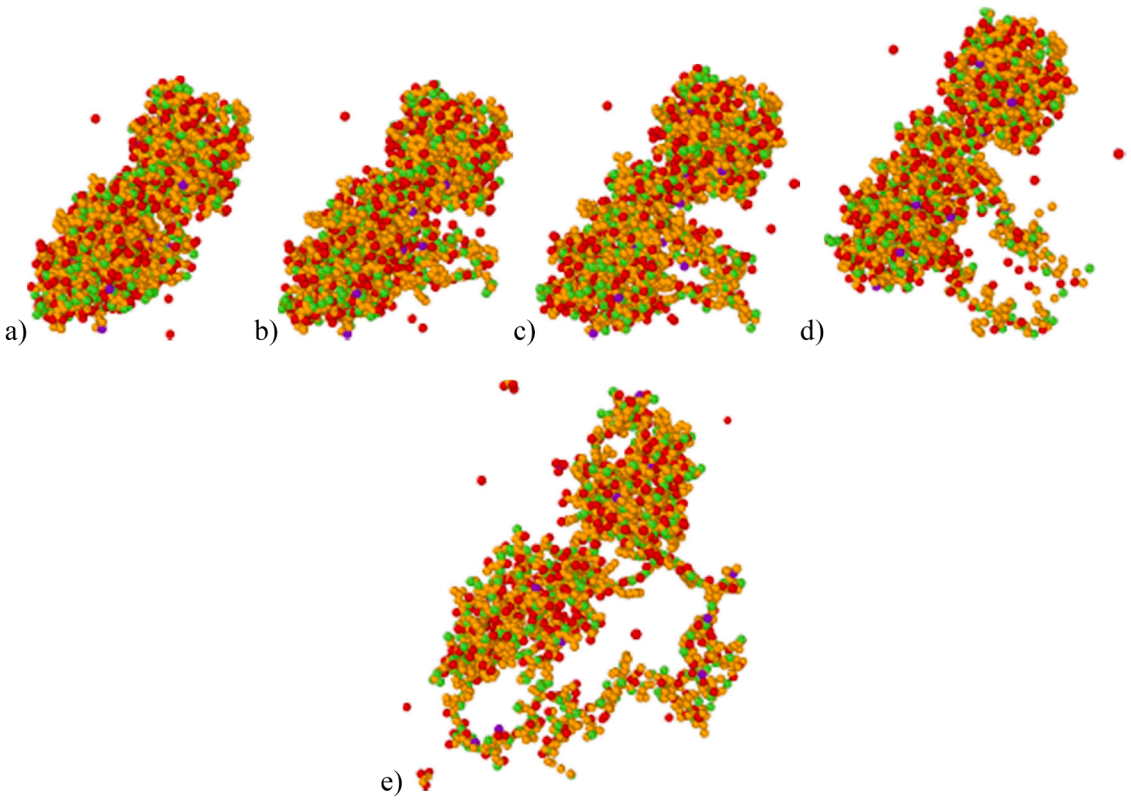

Fig. 2. Structural evolution of the SARS-CoV-2 main protease during the simulation at (a) 0, (b) 25,000, (c) 50,000, (d) 75,000, and (e) 100,000 timesteps.

stability of SARS-CoV-2 under different external conditions [6–10]. Although these works provided useful information about virus persistence and transmission, they did not clarify how nanoscale antiviral agents interact with viral structural proteins under externally controlled physical fields. Silver nanoparticles have attracted considerable attention due to their strong physicochemical activity, high surface-to-volume ratio, and ability to interact with biological macromolecules at the molecular scale [11,12]. When dispersed in water, silver nanoparticles form water/silver nanofluids (NFs) whose mobility, interaction energy (IE), and diffusion behavior can be modified by external forces. In particular, an external electric field can influence charged and polar components of the system, alter molecular orientation, and change the transport behavior of water molecules and nanoparticles [13–15]. Therefore, combining silver-based NFs with a variable electric field may provide a controllable means to enhance interactions with viral proteins. However, the combined effect of NF composition and variable electric-field parameters on the structural stability of SARS-CoV-2-related proteins was not sufficiently addressed at the atomic scale.

Molecular dynamics simulation provided a suitable framework for examining such nanoscale mechanisms because it can track atomic displacement, IE, diffusion, and structural response under controlled thermodynamic and field conditions [16–18]. Several molecular dynamics studies investigated NF transport, electric-field-driven nanoscale behavior, and virus-related molecular interactions [19–22]. Nevertheless, a clear gap remained in understanding how the amplitude and

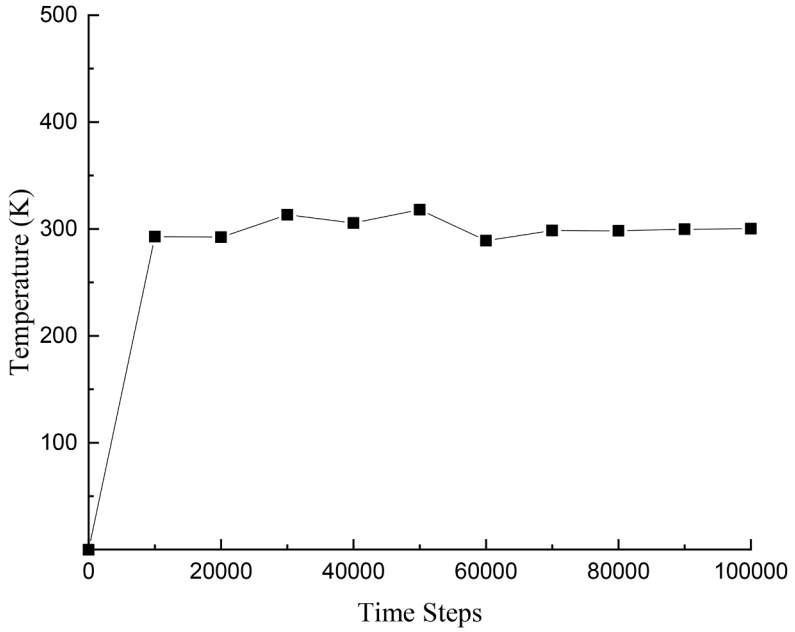

a)

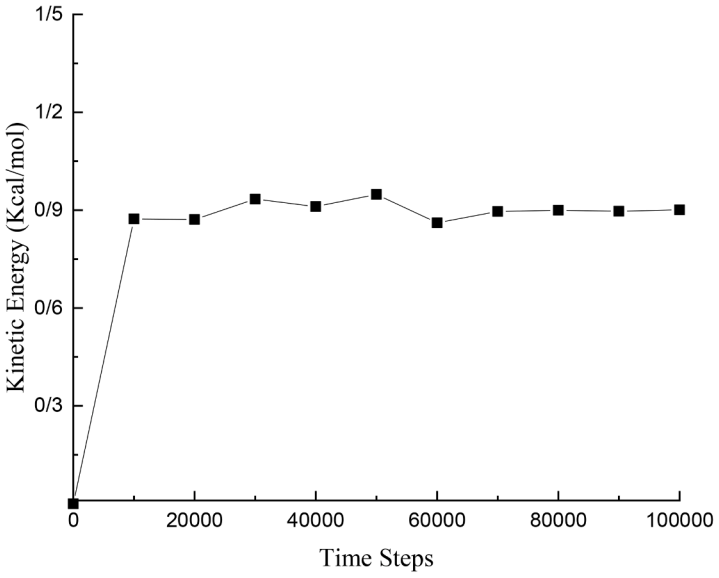

b)

Fig. 3. Equilibration analysis of the simulated system: (a) temperature variation and (b) kinetic energy variation as a function of simulation time.

frequency of an externally applied electric field simultaneously affected the interaction between water/silver NFs and SARS-CoV-2 viral proteins. This gap was important because the electric-field amplitude controlled the intensity of the external force acting on polar or charged species, while the electric-field frequency determined how rapidly the field direction or magnitude changed over time.

Accordingly, the present study employed molecular dynamics simulation to investigate the interaction between a water/silver NF and the SARS-CoV-2 main protease (PDB ID: 7RN1) under variable electric-field conditions. The electric-field amplitude varied from 0.1 to 0.5 V/Å, while the electric-field frequency ranged from 0.01 to 0.04 fs^{-1}. These ranges were selected to systematically evaluate how field strength and oscillation frequency influence atomic mobility, intermolecular interactions, and the protease's structural response. The primary evaluated parameters were the mean-squared displacement (MSD), the diffusion coefficient, and the IE. The MSD and diffusion coefficient characterized the mobility and transport behavior of atoms and nanoparticles, whereas the IE showed the strength and stability of molecular interactions between the NF and the viral protease. The main objective of this work was to determine whether increasing the electric-field amplitude enhanced NF mobility and induced structural perturbations in the SARS-CoV-2 main protease, and whether increasing the field frequency modifies or suppresses these effects. By linking silver NF dynamics to electric-field-controlled molecular motion, this study provided atomistic insight into the mechanisms governing NF–protein systems under external electric fields. It should be noted that the present simulations were limited to the SARS-CoV-2 main protease and did not represent the complete viral particle. Therefore, the findings should be

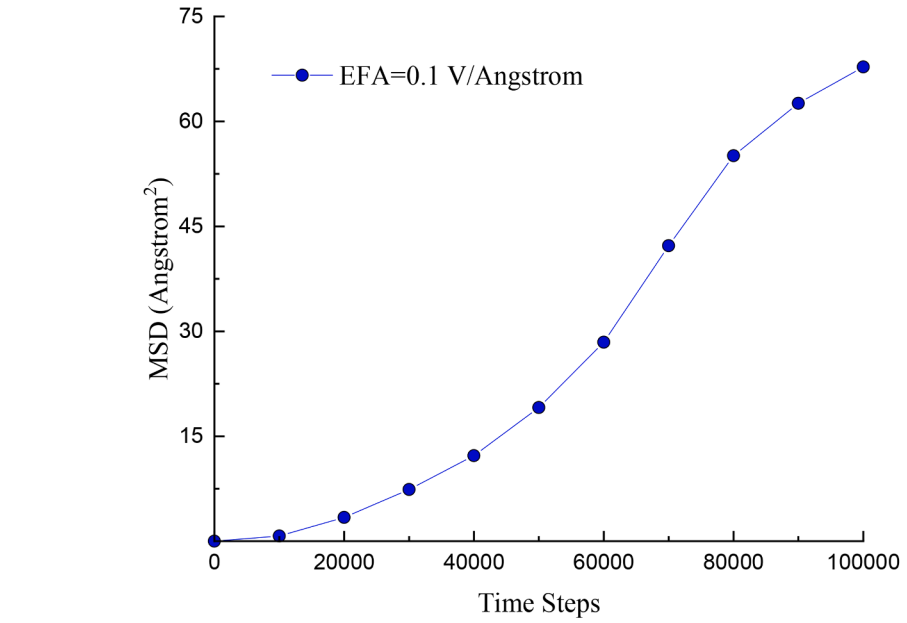

a)

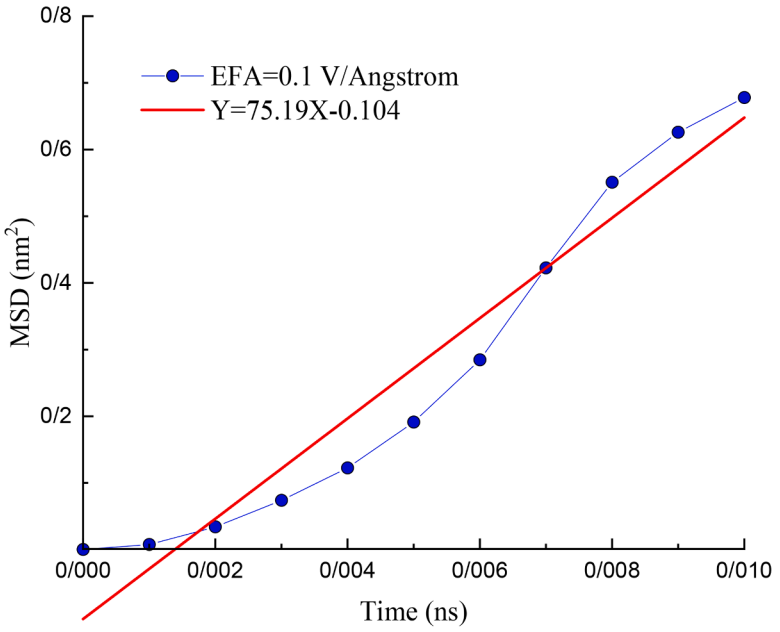

b)

Fig. 4. Variations of (a) MSD and (b) diffusion coefficient of the simulated system at an EFA of 0.1 V/Å.

interpreted as protein-level responses rather than direct evidence of whole-virus inactivation. Nevertheless, the findings contributed to a better understanding of electrically assisted NF–protein interactions and may support the future development of nanoscale antiviral technologies.

2. Numerical method

2.1. Simulation details

All molecular dynamics simulations were done using the Large-scale Atomic/Molecular Massively Parallel Simulator (LAMMPS) package. The crystallographic structure of the SARS-CoV-2 main protease (Mpro) in complex with the inhibitor Juyn9–62–2R (PDB ID: 7RN1) was retrieved from the Protein Data Bank and used as the protein model for molecular dynamics simulations [23]. The viral protein was combined with water molecules and silver nanoparticles generated using Avogadro software [24]. The final simulation system consisted of 9020 atoms, including 600 Ag atoms, 1531 C atoms, 1 Cl atom, 4000 H atoms, 402 N atoms, 2463 O atoms, and 23 S atoms. The solvent phase contained 2000 water molecules. The simulation box dimensions were approximately $145 \times 146 \times 146$ Å^3 with periodic boundary conditions used in all three spatial directions. Interatomic interactions were described utilizing a

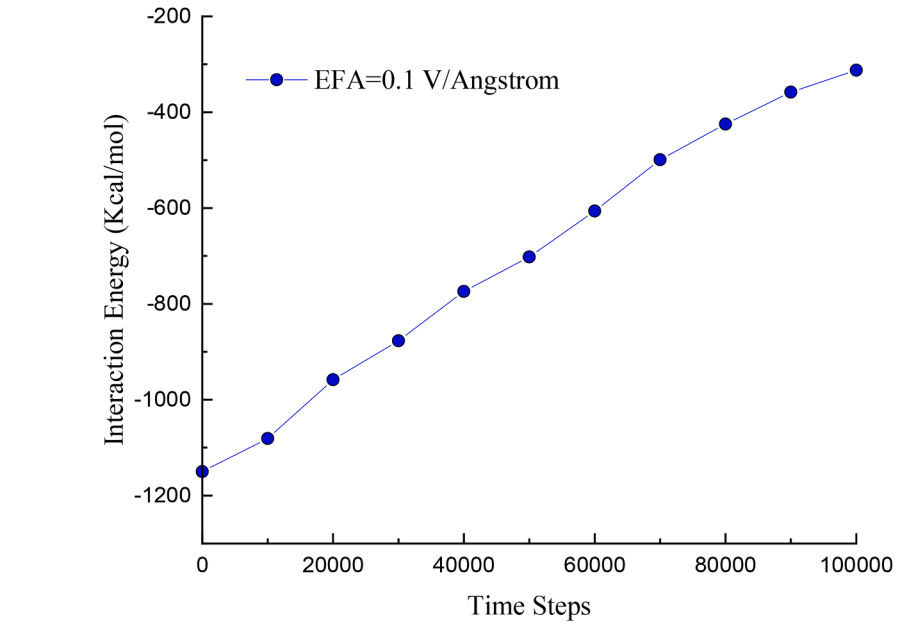

a)

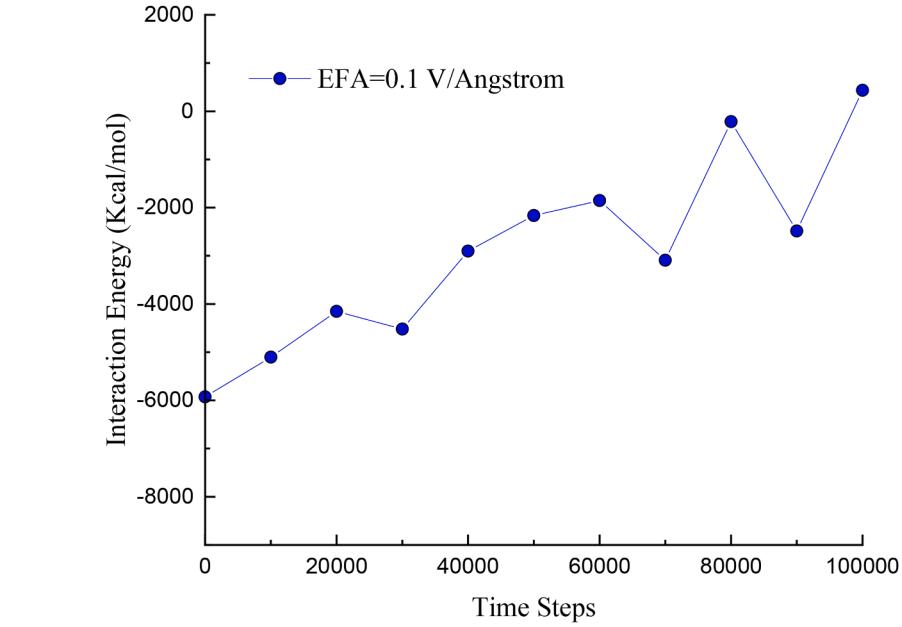

b)

Fig. 5. Variations of the IE between (a) the SARS-CoV-2 main protease and the nanofluid, and (b) different regions of the SARS-CoV-2 main protease at an EFA of 0.1 V/Å.

Lennard–Jones potential with a cutoff distance of 12 Å, together with harmonic bond, angle, and dihedral potentials. Before production calculations, the system was energy-minimized using the conjugate gradient algorithm. Initial atomic velocities were assigned at 300 K. Equilibration was subsequently performed in the canonical (NVT) ensemble applying a Nose–Hoover thermostat to maintain the system temperature at 300 K. A timestep of 0.1 fs was employed throughout the simulations. The equilibration stage was carried out for 100,000 timesteps, corresponding to 10 ps. Equilibrium was confirmed through stabilization of both the kinetic energy and temperature profiles. Following equilibration, the thermostat was removed, and the simulations were continued in the microcanonical (NVE) ensemble for an additional 100,000 timesteps (10 ps). The external electric field was implemented using the LAMMPS efield command according to a sinusoidal function:

$$E(t) = E_0 sin(\omega t) \quad (1)$$

where E_o denotes the electric-field amplitude, and ω is the frequency parameter. The electric field was applied simultaneously along with x-, y-, and z-directions. The electric-field amplitude was varied between 0.1

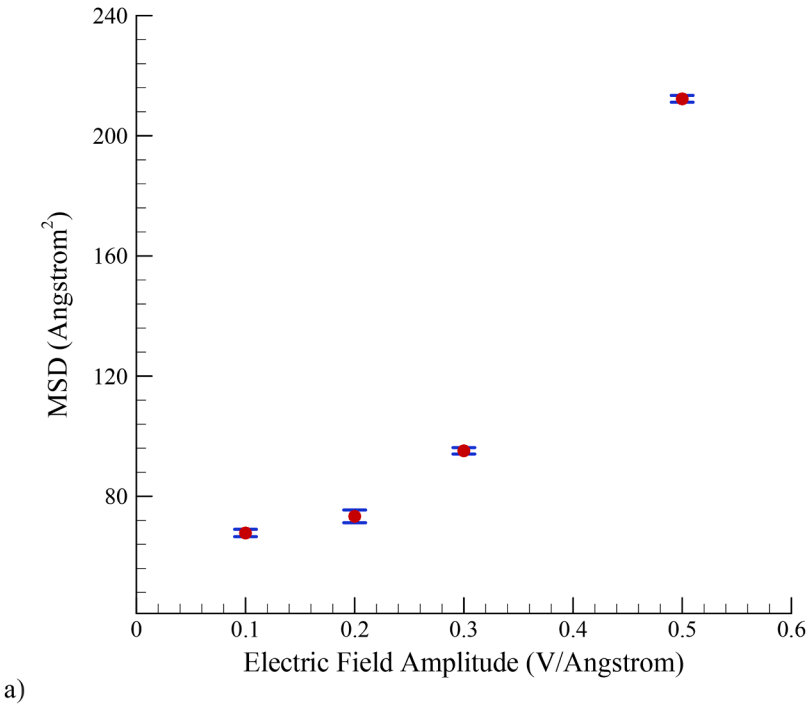

a)

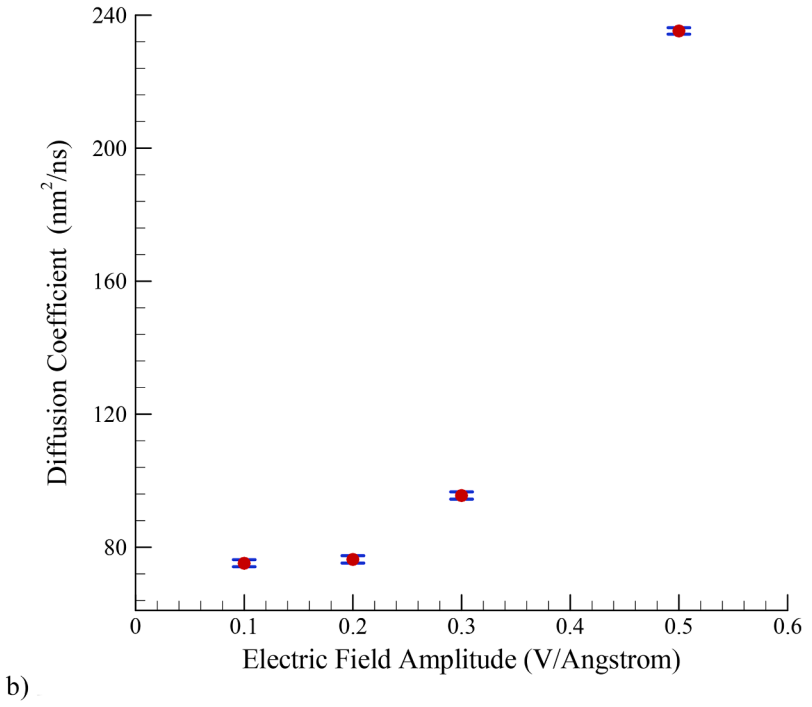

b)

Fig. 6. Variations of (a) MSD and (b) diffusion coefficient of the simulated system at different EFAs.

and 0.5 V/Å, while the frequency parameter ranged from 0.01 to 0.04 fs^{-1}. The mean squared displacement, diffusion coefficient, and IE were subsequently calculated to evaluate NF mobility and virus–NF interactions under different electric-field conditions. The prototype structures modeled are illustrated in Fig. 1. Additionally, the viral eradication process, which concluded the current computational investigation, is depicted in Fig. 2.

2.2. Equilibrium process

The equilibrium stage of the modeled system, in the absence of an external electric field, served as the initial state of the present molecular dynamics investigation. To evaluate the system's stability and verify the adequacy of the simulation conditions, the temperature and kinetic energy profiles were monitored over simulation time [21,25]. As shown in Fig. 3a, the system temperature gradually approached the target value of 300 K and remained stable after approximately 100,000 timesteps. This behavior showed the progressive redistribution of atomic velocities

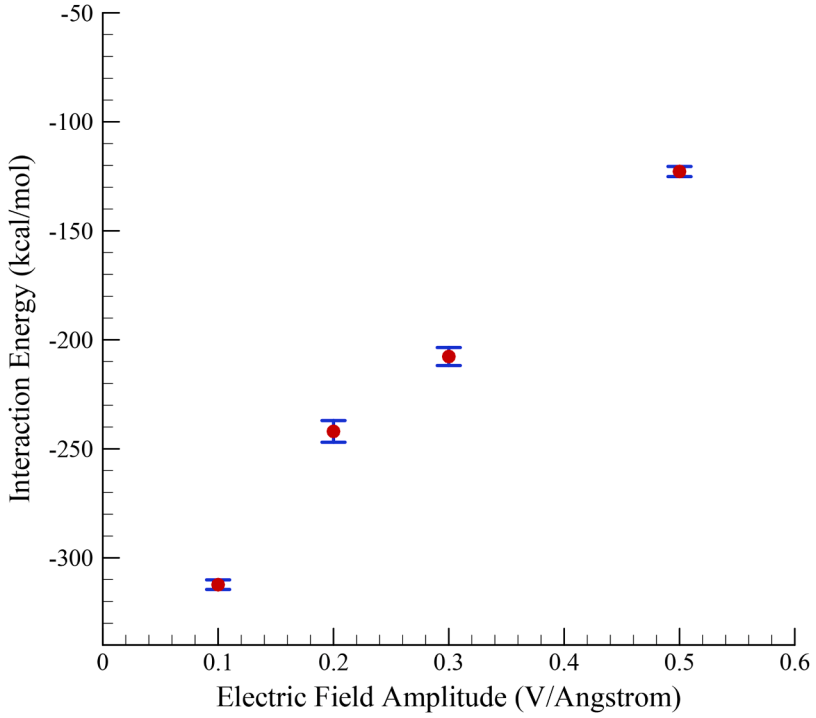

Fig. 7. Variations of the IE between the SARS-CoV-2 main protease and the nanofluid at different EFAs.

Table 1
The numerical changes in MSD, diffusion coefficient, and IE of the SARS virus at different EFAs.

EFA (V/Å)	MSD (Å^2)	D (nm^2/ns)	IE (kcal/mol)	
			SARS-Naofluid	SARS-SARS
0.1	67.78 (±1.23)	75.19 (±1.06)	−312.32 (±2.21)	−435.82 (±20.87)
0.2	73.32 (±2.12)	76.34 (±1.11)	−242.01 (±4.98)	−1583.79 (±21.41)
0.3	95.14 (±1.07)	95.55 (±1.09)	−207.68 (±4.11)	−1923.56 (±22.55)
0.5	212.3 (±1.14)	235.25 (±0.98)	−122.80 (±2.33)	−659.43 (±18.83)

and the attainment of thermal equilibrium within the simulation box. The evolution of kinetic energy provided additional evidence of system stabilization. As illustrated in Fig. 3b, the kinetic energy converged to approximately 0.901 kcal/mol at the end of the equilibration stage. The simultaneous stabilization of both temperature and kinetic energy indicated that the modeled system reached a thermodynamically stable state suitable for subsequent analyses [26]. Therefore, the equilibration procedure confirmed the consistency of initial atomic configuration, interaction parameters, and simulation settings employed in the present work.

3. Results and discussion

Following the equilibration stage, the structural response of the water/silver NF–protease system was studied under an external electric field using the NVE ensemble. In the first set of simulations, the electric-field amplitude was fixed at 0.1 V/Å. The atomic mobility of the system was assessed using the mean squared displacement (MSD), which quantified the average squared displacement of atoms over time and provided insight into molecular transport and dynamic behavior within the simulated environment.

As shown in Fig. 4a, the MSD increased continuously throughout the simulation, indicating enhanced atomic motion and increased mobility of NF components surrounding the SARS-CoV-2 main protease. Numerically, the MSD reached 67.78 Å^2 at the final timestep. The corresponding diffusion coefficient, calculated from the MSD data, is shown in Fig. 4b. It converged to 75.19 nm^2/ns, demonstrating significant nanoscale transport activity within the system.

The interaction between NF and the protease was further examined through IE analysis. IE represents the net energetic contribution arising from intermolecular interactions, including van der Waals forces and other nonbonded interactions. Fig. 5a presents the IE between the SARS-CoV-2 main protease and the surrounding NF, whereas Fig. 5b illustrates the IE within the protease structure itself. At the end of the simulation, these interaction energies converged to −312.32 and −435.82 kcal/mol, respectively.

The combined MSD, diffusion coefficient, and interaction-energy results suggested that the external electric field promoted enhanced NF mobility and modified the interaction behavior between NF and the protease. These changes indicated increasing structural perturbations at the protein level and demonstrated the sensitivity of SARS-CoV-2 main protease to externally controlled NF dynamics. However, since the present model represented only the main protease rather than the complete viral particle, the observed effects should be interpreted as protein-level structural responses rather than direct evidence of whole-virus inactivation.

3.1. Electric field amplitude magnitude

In this section, the amplitude of the electric field (EFA) was increased from 0.1 to 0.5 V/Å, and the changes in the MSD and diffusion coefficient were discussed. Fig. 6 shows the change in MSD and diffusion coefficient with respect to EFA. From the graph, it is clear that with increasing EFA, the MSD and diffusion coefficient increased significantly, and at EFA = 0.5 V/Å, the MSD and diffusion coefficient were 212.30 Å^2 and 235.25 nm^2/ns, respectively. These parameters showed that the atomic mobility in water/silver NF-protease mixture was enhanced at higher electric-field strength. This effect was due to enhanced interaction of the electric field with the charged or polarizable

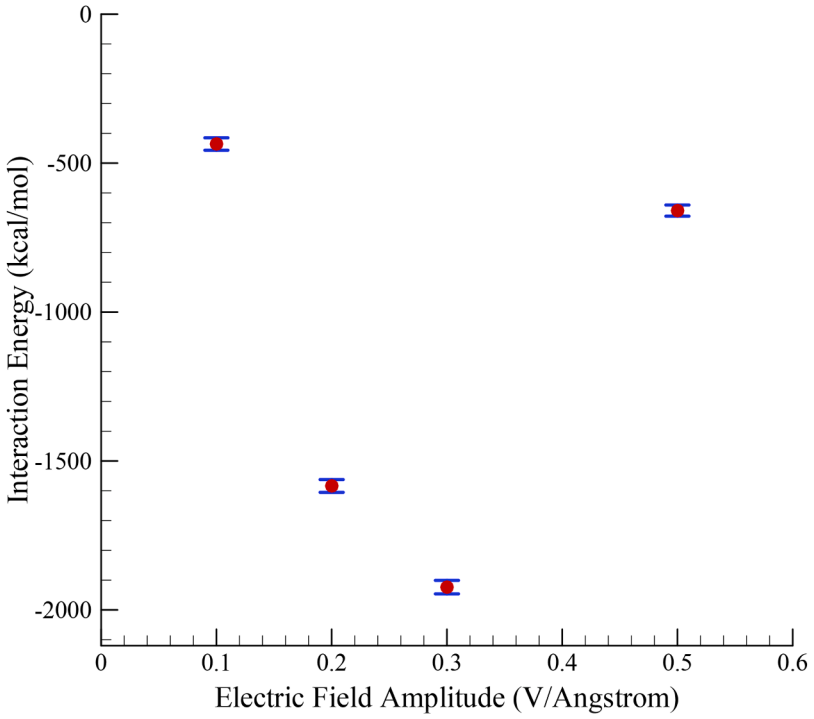

Fig. 8. Variations of the IE within the SARS-CoV-2 main protease structure at different EFAs.

particles in the medium. As EFA increased, the electric field exerted a greater force on atoms and molecules, thereby enhancing their mobility. In addition, the electric field influenced the orientation of water molecules and polar functional groups within the protease, modifying local interaction patterns and facilitating nanoscale transport. Consequently, both the MSD and diffusion coefficient increased significantly with increasing EFA, demonstrating the important role of electric-field intensity in controlling molecular mobility and transport behavior.

The IE between the NF and the SARS-CoV-2 main protease at different EFAs is presented in Fig. 7. As the EFA increased from 0.1 to 0.5 V/Å, the IE changed from −312.32 to −122.80 kcal/mol. The shift toward less negative values indicated a reduction in the magnitude of attractive interactions between the NF and the protease. This behavior proposed that the stronger electric field enhanced atomic mobility and dynamic fluctuations, thereby weakening the energetic favorability of protease–NF interactions. The reduced magnitude of IE was consistent with the increased MSD and diffusion coefficient values observed at higher EFAs, indicating that stronger electric fields promoted greater molecular motion while reducing interaction stability. Together, the MSD, diffusion coefficient, and interaction-energy results demonstrated that increasing the electric-field amplitude enhanced atomic mobility and significantly modified the interaction behavior between the water/silver NF and the SARS-CoV-2 main protease. The combination of increased transport activity and reduced interaction stability suggested increasing structural perturbations at the protein level. However, because the present model represented only the SARS-CoV-2 main protease rather than the complete viral particle, these findings should be interpreted as changes in protease stability and interaction behavior rather than direct evidence of whole-virus disruption or inactivation. Table 1 summarizes the numerical values of MSD, diffusion coefficient, and IE obtained at different electric-field amplitudes.

Fig. 8 presents the variation of IE within the SARS-CoV-2 main protease at different electric-field amplitudes. The results reveal a nonlinear dependence of the intramolecular IE on the applied electric field. At intermediate EFAs (0.2 and 0.3 V/Å), the IE became more negative, indicating stronger attractive intramolecular interactions and a relatively more stable energetic configuration. This behavior may be attributed to field-induced reorientation of polar groups and redistribution of local atomic interactions within the protease. However, when the EFA increased to 0.5 V/Å, the IE shifted toward a less negative value (−659.43 kcal/mol), indicating a reduction in the strength of stabilizing intramolecular interactions. At high field intensities, enhanced atomic mobility and larger structural fluctuations altered the protein's interaction network, reducing the energetic stability of the protease structure. As a result, the stabilizing effect observed at intermediate EFAs was partially lost under stronger electric-field conditions.

3.2. *The electric field frequency magnitude*

In this section, an external electric field with an amplitude of 0.4 V/Å and a frequency parameter of 0.01 fs^{-1} was applied to the simulated system. Fig. 9 presents the variations in the mean-squared displacement (MSD) and the diffusion coefficient as functions of simulation time. The corresponding numerical values of MSD, diffusion coefficient, and IE at different electric-field frequencies (EFFs) are summarized in Table 2.

Fig. 9 presents the changes in MSD and the diffusion coefficient as functions of simulation time at an electric-field amplitude of 0.4 V/Å and a frequency of 0.01 fs^{-1}. The results indicate that the MSD and diffusion coefficient increased continuously during the simulation and reached 158.61 $Å^2$ and 141.19 nm^2/ns, respectively, at the final time-step. These values demonstrated significant atomic mobility and transport activity within the water/silver NF–protease system under the applied electric field. The observed behavior can be attributed to the oscillating electric field, which exerted periodic forces on charged and polarizable species throughout the simulation domain. These forces promoted atomic displacements, molecular reorientation, and enhanced transport of NF components. As a result, larger average atomic displacements were observed, leading to increased MSD values. Similarly, the higher diffusion coefficient indicated more efficient molecular transport and greater mobility of NF particles surrounding the protease. The continuous oscillation of the electric field dynamically modified the local interaction environment by repeatedly perturbing intermolecular interactions and molecular orientations. This process enhanced atomic motion and facilitated nanoscale transport throughout the system.

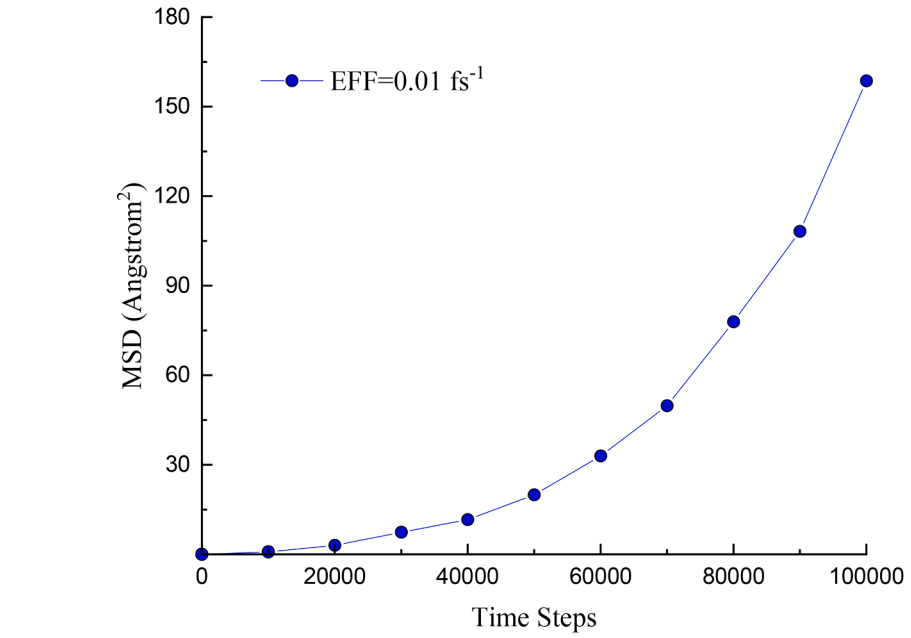

a)

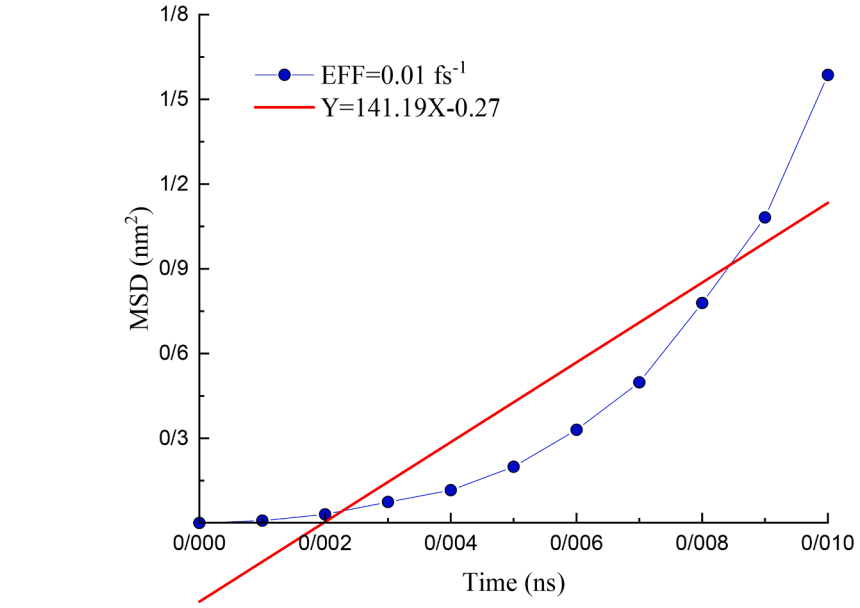

b)

Fig. 9. Variations of (a) MSD and (b) diffusion coefficient of the simulated system at an EFF of 0.01 fs^{-1}.

Consequently, the elevated MSD and diffusion-coefficient values indicated that the applied electric field significantly influenced molecular mobility and interaction dynamics within the water/silver NF–protease system.

Fig. 10 presents the variation in IE between the SARS-CoV-2 main protease and the surrounding NF (Fig. 10a), as well as the IE within the protease structure itself (Fig. 10b). After 100,000 timesteps, the protease–NF IE and the intramolecular protease IE reached 3420.76 and −83.14 kcal/mol, respectively. The highly positive protease–NF IE indicated that the interaction environment became energetically unfavorable under applied electric-field conditions. This behavior suggested that the oscillating electric field significantly altered the relative arrangement of NF components and protein atoms, resulting in increased atomic mobility and reduced energetic compatibility between the interacting species. Simultaneously, the relatively weak negative value of the intramolecular protease IE indicated that the stabilizing interactions within the protein were weaker than those in more energetically favorable configurations. These energetic characteristics were consistent with the elevated MSD and diffusion coefficient values observed in Fig. 9, indicating enhanced molecular motion throughout the system. The combination of high atomic mobility and energetically unfavorable protease–NF interactions suggested that the applied electric field induced substantial dynamic perturbations within the protein environment. Consequently, the interaction behavior and energetic

Table 2
The numerical changes in MSD, diffusion coefficient, and IE of the SARS virus at different EFFs.

EFF (fs^{-1})	MSD ($Å^2$)	D (nm^2/ns)	IE (Kcal/mol)	
			SARS-Naofluid	SARS-SARS
0.01	158.61 (±1.24)	141.19 (±1.12)	−83.14 (±3.32)	3420.76 (±21.21)
0.02	93.023 (±1.51)	94.62 (±1.05)	−245.71 (±3.12)	−973.79 (±20.47)
0.03	79.33 (±1.48)	88.92 (±1.07)	−262.29 (±4.91)	−2913.76 (±19.87)
0.04	65.67 (±1.03)	68.94 (±0.98)	−259.35 (±4.04)	−1726.03 (±19.41)

stability of SARS-CoV-2 main protease were strongly influenced by the external electric field. However, because the present model represented only SARS-CoV-2 main protease rather than the complete viral particle, these findings should be interpreted as protein-level energetic and structural responses rather than direct evidence of whole-virus disruption or inactivation.

Fig. 11 presents the variations of MSD and diffusion coefficient as the electric-field frequency (EFF) increased from 0.01 to 0.04 fs^{-1}. The results show that the MSD and diffusion coefficient decreased from 158.61 $Å^2$ and 141.19 nm^2/ns to 65.67 $Å^2$ and 68.94 nm^2/ns, respectively, as EFF increased. These results indicate that higher electric-field frequencies suppressed atomic mobility within the water/silver NF–protease system. Physically, the decrease in MSD was reflected in smaller average atomic displacements and reduced molecular motion throughout the simulation domain. Similarly, the reduced diffusion coefficient indicated less efficient transport of the NF components under rapidly oscillating electric-field conditions. At higher frequencies, the electric field changed direction more rapidly than the characteristic response time of the atoms and molecules. Consequently, NF components and protein atoms could not fully align with or respond to each oscillation cycle. This dynamic lag reduced the net displacement induced by the field and limited long-range transport within the system. As a result, atomic mobility and diffusion decreased as the electric-field frequency increased. This behavior was consistent with the concept that rapidly oscillating fields reduced the effectiveness of field-driven molecular motion by continuously reversing the direction of applied force before significant displacement could occur [27,28].

Fig. 12 illustrates the variation of IE between the SARS-CoV-2 main protease and the surrounding NF at different electric-field frequencies. The IE decreased from −83.14 kcal/mol to −259.35 kcal/mol as the EFF increased from 0.01 to 0.04 fs^{-1}. The shift toward more negative values indicated stronger attractive interactions between the protease and NF components. Unlike the effect of increasing the electric-field amplitude, which weakened the interaction strength, increasing the electric-field frequency promoted a more energetically favorable interaction environment. The stronger attractive interactions observed at higher frequencies were consistent with the reduced atomic mobility indicated by the MSD and diffusion coefficient results. Because atoms experience smaller net displacements at high frequencies, they remain within a more stable interaction environment, leading to more negative interaction energies and enhanced protease–NF interaction stability [29].

Fig. 13 presents the variation of IE within the SARS-CoV-2 main protease at different electric-field frequencies. The corresponding interaction energies were 3420.76, −973.79, −2913.76, and −1726.03 kcal/mol for EFF values of 0.01, 0.02, 0.03, and 0.04 fs^{-1}, respectively. The results reveal a non-monotonic dependence of the intramolecular IE on electric-field frequency. At the lowest frequency, the highly positive IE indicated a strongly perturbed energetic state associated with enhanced molecular motion and dynamic fluctuations. Increasing the frequency to 0.02 and 0.03 fs^{-1} produces substantially more negative interaction energies, indicating stronger stabilizing intramolecular interactions within the protease. This trend was consistent with the reduced atomic mobility observed in the MSD and diffusion-coefficient analyses. However, a further increase to 0.04 fs^{-1} resulted in a partial reduction in the magnitude of IE, suggesting that excessive oscillation frequencies may introduce additional dynamic perturbations that partially offset the stabilizing effect observed at intermediate frequencies.

The combined MSD, diffusion coefficient, and interaction-energy results demonstrated that electric-field frequency played a critical role in regulating atomic mobility and interaction behavior within the water/silver NF–protease system. Lower frequencies promoted greater molecular motion and dynamic fluctuations because the atoms can respond more effectively to the applied field. In contrast, higher frequencies suppressed atomic mobility by limiting the ability of atoms and molecules to follow the rapidly oscillating electric field. This reduction in mobility was accompanied by more negative interaction energies, indicating stronger attractive interactions and greater energetic stability within the system. Therefore, unlike increasing the electric-field amplitude, which enhanced mobility and promoted structural perturbation, increasing the electric-field frequency tended to stabilize protein–NF interactions by reducing field-driven transport. These findings highlighted the sensitivity of SARS-CoV-2 main protease to electric-field frequency and demonstrated the important role of frequency in controlling nanoscale protein–NF interactions. Because the present model included only SARS-CoV-2 main protease, these observations should be interpreted as protein-level responses rather than direct evidence of whole-virus behavior or inactivation [30–32].

4. Conclusion

The present study demonstrated that the amplitude and frequency of an external electric field significantly influenced the interaction behavior and dynamic response of a water/silver NF–SARS-CoV-2 main protease system. Molecular dynamics simulations showed that increasing the electric-field amplitude from 0.1 to 0.5 V/Å increased the diffusion coefficient from 75.19 to 235.25 nm^2/ns and changed the protease–NF IE from −312.32 to −122.80 kcal/mol, indicating enhanced atomic mobility and modified intermolecular interactions under stronger electric-field conditions. In contrast, increasing the electric-field frequency from 0.01 to 0.04 fs^{-1} at a fixed amplitude of 0.4 V/Å decreased the diffusion coefficient from 141.19 to 68.94 nm^2/ns and changed the IE from −83.14 to −259.35 kcal/mol, indicating reduced atomic mobility and stronger attractive interactions within the system. These findings demonstrated that electric-field amplitude and frequency exert distinct influences on nanoscale transport behavior and protein–NF interactions. Therefore, higher electric-field amplitudes promoted greater molecular mobility and stronger dynamic perturbations, whereas higher frequencies suppressed atomic motion and enhanced interaction stability. The results provided atomistic insight into the response of the SARS-CoV-2 main protease to externally controlled NF environments. However, since the present model represented only the SARS-CoV-2 main protease rather than the complete viral particle, the findings should be interpreted as protein-level responses rather than as direct evidence of whole-virus inactivation. Future studies involving additional viral components and larger-scale models are needed further to evaluate the implications of these effects for antiviral applications.

4.1. Limitation

A limitation of the present study was that the molecular model represented only the SARS-CoV-2 main protease (PDB ID: 7RN1) rather than the complete viral particle. Consequently, the observed structural perturbations and interaction changes should be interpreted as protein-level responses to the combined effects of water/silver NFs and external electric fields. Additional studies involving other viral proteins, larger biomolecular assemblies, or multiscale modeling approaches are

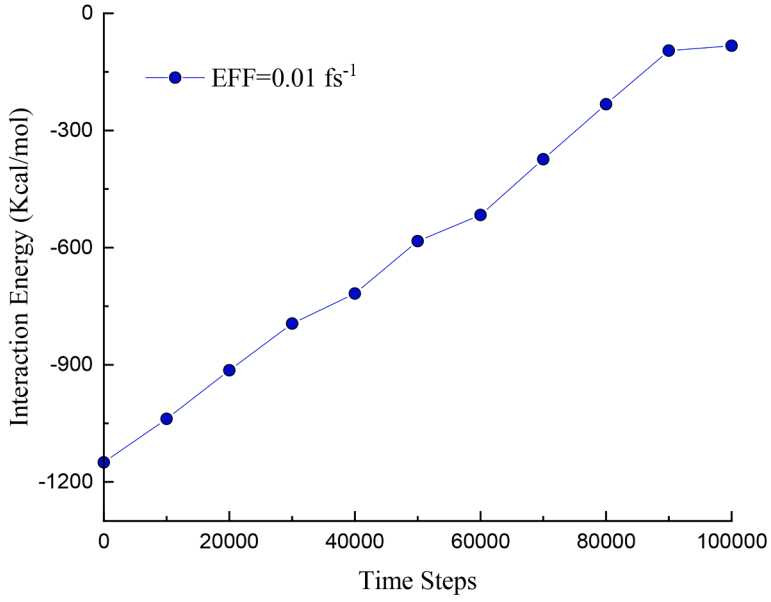

a)

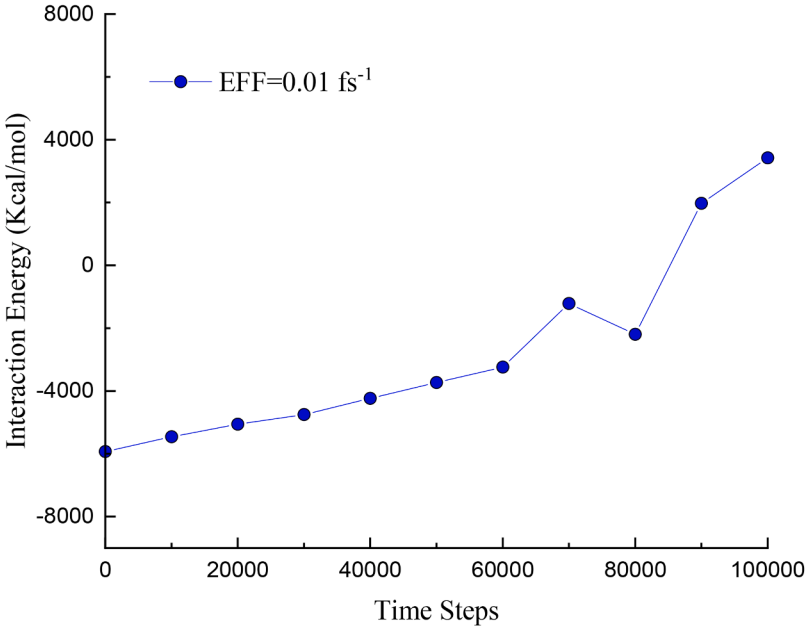

b)

Fig. 10. Variations of the IE between (a) the SARS-CoV-2 main protease and the nanofluid, and (b) different regions of the SARS-CoV-2 main protease at an EFF of 0.01 fs^{-1}.

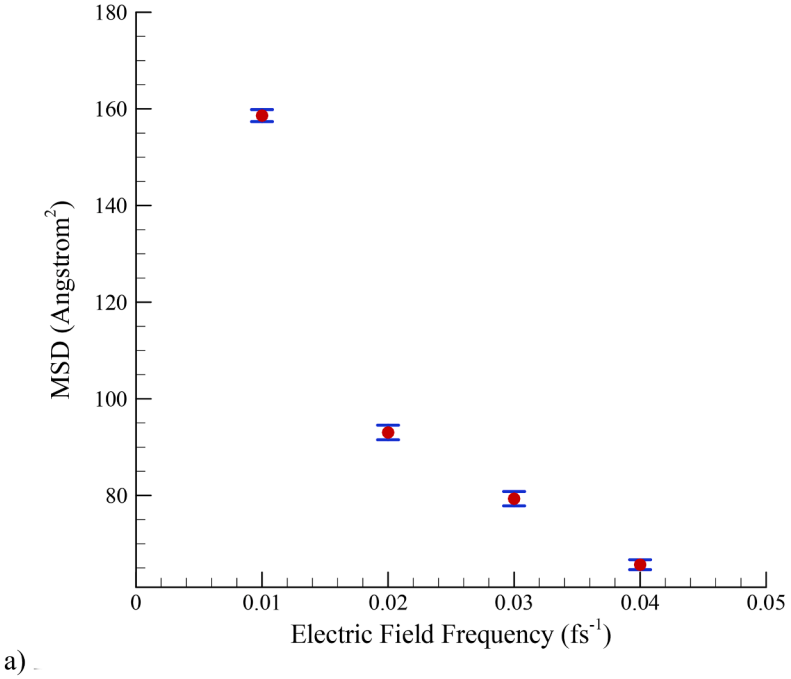

a)

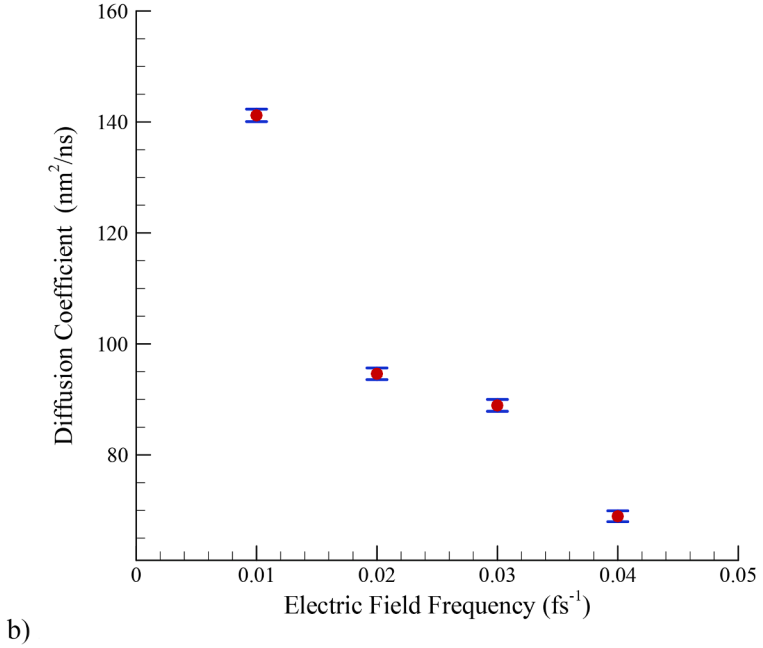

b)

Fig. 11. Variations of (a) MSD and (b) diffusion coefficient of the simulated system at different EFFs.

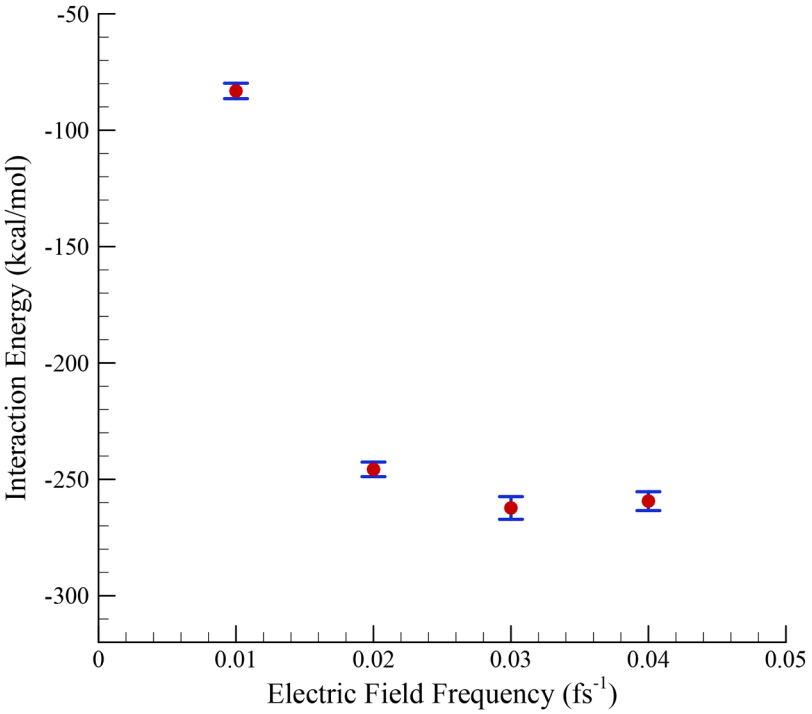

Fig. 12. Variations of the IE between the SARS-CoV-2 main protease and the nanofluid at different EFFs.

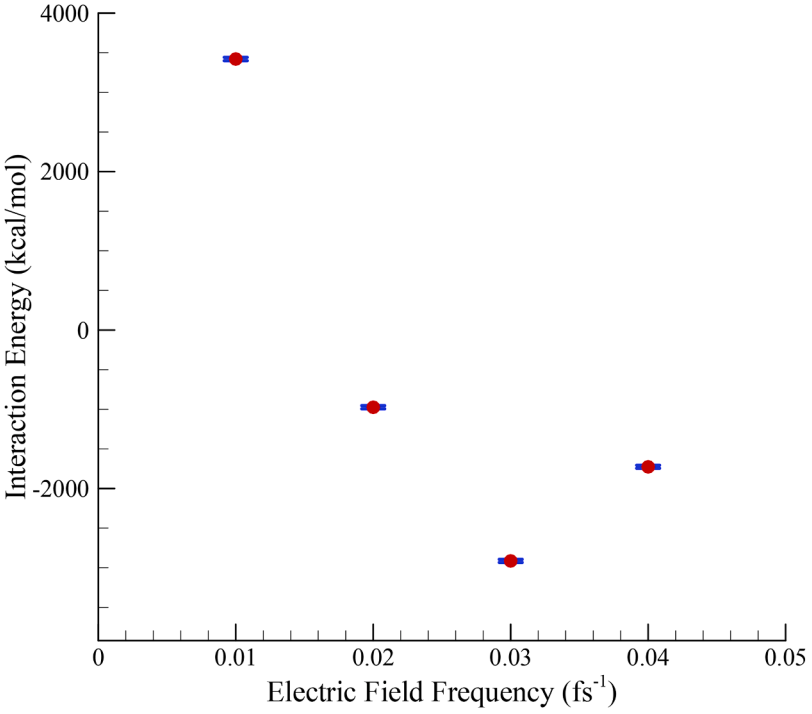

Fig. 13. Variations of the IE within the SARS-CoV-2 main protease structure at different EFFs.

required before extending these findings to whole-virus behavior or virus inactivation mechanisms.

Clinical trial number

Not applicable.

Funding source

Not applicable.

CRediT authorship contribution statement

Ali Alkhafaji: Conceptualization, Formal analysis, Writing – original draft. **Ahmed Mohammed Attyah Zheoat:** Conceptualization, Investigation, Supervision, Project administration, Funding acquisition. **Mohammed R. Hashim Al-Dahhan:** Methodology, Data curation, Writing – original draft, Funding acquisition, Supervision. **Narinderjit Singh Sawaran Singh:** Methodology, Validation, Resources, Writing – original draft, Visualization, Project administration. **Banaz Shahab Haji:** Software, Validation, Project administration, Funding acquisition. **Hakim AL Garalleh:** Software, Resources, Visualization. **Zuhair Jastaneyah:** Formal analysis, Visualization, Funding acquisition. **Soheil Salahshour:** Methodology, Investigation, Visualization, Funding acquisition. **Mahmut Taner:** Software, Validation, Formal analysis, Data curation, Writing – original draft, Funding acquisition, Writing – original draft.

Declaration of competing interest

The authors declare that they have no known competing financial interests or personal relationships that could have appeared to influence the work reported in this paper.

Acknowledgments

N/A.

Data availability

No data was used for the research described in the article.

References

[1] C.M. Zmasek, E.J. Lefkowitz, A. Niewiadomska, R. Scheuermann, Genomic evolution of the Coronaviridae family, Virology 570 (2022) 123–133.
[2] N.I. Borisova, I.A. Kotov, A.A. Kolesnikov, V.V. Kaptelova, A.S. Speranskaya, L. Y. Kondrasheva, E.V. Tivanova, K.F. Khafizov, V. Akimkin, Monitoring the spread of the SARS-CoV-2 (Coronaviridae: coronavirinae: betacoronavirus; Sarbecovirus) variants in the Moscow region using targeted high-throughput sequencing, Probl. Virol. 66 (4) (2021) 269–278.
[3] M. Hasöksüz, S. Kilic, F. Saraç, Coronaviruses and sars-cov-2, Turk. J. Med. Sci. 50 (9) (2020) 549–556.
[4] C. Sathyaseelan, M.A. Magateshvaren Saras, L.P. Prasad Patro, P.P. Uttamrao, T. Rathinavelan, CoVe-tracker: an interactive SARS-CoV-2 pan proteome evolution tracker, J. Proteome. Res. 22 (6) (2023) 1984–1996.
[5] S. Ludwig, A.J Zarbock, Analgesia, Coronaviruses and SARS-CoV-2: a brief overview, Anesth. Analg. 131 (1) (2020) 93–96.
[6] J.J. Guadalupe, M.I. Rojas, G. Pozo, M.P. Erazo-Garcia, P. Vega-Polo, M. Terán-Velástegui, F. Rohwer, M.D.L. Torres, Presence of SARS-CoV-2 RNA on surfaces of public places and a transportation system located in a densely populated urban area in South America, Viruses 14 (1) (2021) 19.
[7] T. Borisova, S. Komisarenko, Air pollution particulate matter as a potential carrier of SARS-CoV-2 to the nervous system and/or neurological symptom enhancer: arguments in favor, Environmental Science and Pollution Research 28 (2021) 40371–40377.
[8] N. Akhtar, N. Nawaz, S. BiBi, M. Ahmad, Impact of climatic factors on viability of SARS-CoV-2 and transmission prospective of COVID-19: an overview, Microbes and Infectious Diseases 1 (3) (2020) 118–125.
[9] S. Chowdhury, M. Forkan, S.F. Ahmed, P. Agarwal, A.S. Ali, S. Muyeen, Modeling the SARS-CoV-2 parallel transmission dynamics: asymptomatic and symptomatic pathways, Comput. Biol. Med. 143 (2022) 105264.
[10] L. Mohammadi, A. Mehravaran, Z. Derakhshan, E. Gharehchahi, E. Bontempi, M. Golaki, R. Khaksefidi, M. Motamed-Jahromi, M. Keshtkar, A. Mohammadpour, Investigating the role of environmental factors on the survival, stability, and transmission of SARS-CoV-2, and their contribution to COVID-19 outbreak: a review, Sustainability 14 (18) (2022) 11135.
[11] X.-F. Zhang, Z.-G. Liu, W. Shen, S. Gurunathan, Silver nanoparticles: synthesis, characterization, properties, applications, and therapeutic approaches, Int. J. Mol. Sci. 17 (9) (2016) 1534.
[12] M.K. Rai, S. Deshmukh, A. Ingle, A. Gade, Silver nanoparticles: the powerful nanoweapon against multidrug-resistant bacteria, J. Appl. Microbiol. 112 (5) (2012) 841–852.
[13] Y. Huang, Z. Zeng, R. Chen, T. Wang, Z. Che, Molecular dynamics study of ammonia poisoning in proton exchange membrane with electric field, J. Power Sourc. 663 (2026) 238870.
[14] Y. Zhao, X. Yang, X. Ye, Z. Fan, S. Li, Y. He, Z. Lu, D. Musinguzi, Molecular dynamics study on the influence of electric field on the wetting behavior of nanoscale water droplets on PDMS surface, Computat. Mater. Sci. 261 (2026) 114321.
[15] B. Roux, The membrane potential and its representation by a constant electric field in computer simulations, Biophys. J. 95 (9) (2008) 4205–4216.
[16] L. Wang, X. Gu, Y. Zhao, J. Tian, X. Ma, M. Tong, Advances in molecular dynamics simulations for hydrogels and nanocomposite-reinforced hydrogels: multiscale simulation strategies and future directions, Gels 12 (4) (2026) 288.
[17] R. Ishraaq, S. Das, All-atom molecular dynamics simulations of polymer and polyelectrolyte brushes, Chem. Commun. 60 (48) (2024) 6093–6129.
[18] K. Joll, P. Schienbein, K.M. Rosso, J. Blumberger, Molecular dynamics simulation with finite electric fields using perturbed neural network potentials, Chem. Phys. (2024).
[19] I.S. Gataa, B.A. Hussein, S.M. Sajadi, H.A. Aljaafari, S. Salahshour, S. Baghaie, The influence of initial temperature on the interactions of water/silver nanofluid with SARS virus using molecular dynamics simulation, Powd. Techn. (2025) 121429.
[20] L. Xiao, A. Basem, Y. Zhang, D.J. Jasim, S. Salahshour, Z. Li, D.J. Toghraie, A numerical study of the effect of variable heat flux on the stability and thermal behavior of SARS-COV-2 structure: a molecular dynamics approach, Case Stud. Therm. Engineer. 56 (2024) 104213.
[21] N.S.S. Singh, I.S. Gataa, S.H. Mohammed, S. Salahshour, S.M. Sajadi, H. Sahramaneshi, Investigating the effect of the atomic ratio of ClO2 gas on the disinfection process of the influenza virus using molecular dynamics simulation, Results Engineer. (2025) 107175.
[22] A. Asgari, Q. Nguyen, A. Karimipour, Q.-V. Bach, M. Hekmatifar, R. Sabetvand, Investigation of additives nanoparticles and sphere barriers effects on the fluid flow inside a nanochannel impressed by an extrinsic electric field: a molecular dynamics simulation, J. Mol. Liq. 318 (2020) 114023.
[23] C. Ma, Z. Xia, M.D. Sacco, Y. Hu, J.A. Townsend, X. Meng, J. Choza, H. Tan, J. Jang, M. Gongora, Discovery of di-and trihaloacetamides as covalent SARS-CoV-2 main protease inhibitors with high target specificity, J. Am. Chem. Soc. 143 (49) (2021) 20697–20709.
[24] M.D. Hanwell, D.E. Curtis, D.C. Lonie, T. Vandermeersch, E. Zurek, G.R. Hutchison, Avogadro: an advanced semantic chemical editor, visualization, and analysis platform, J. Cheminform. 4 (2012) 1–17.
[25] L. Verlet, Computer experiments" on classical fluids. I. Thermodynamical properties of Lennard-Jones molecules, Phys. Rev. 159 (1) (1967) 98.
[26] W.T. Vetterling, S.A. Teukolsky, W.H. Press, B.P. Flannery, Numerical Recipes in C: the Art of Scientific Computing, Cambridge University Press, 1999.
[27] D. Wu, A.B. Ali, A.A. Mohammed, A. Alizadeh, S. Salahshour, M. Hashemian, M. Wang, The stability of the SARS-COV-2 structure in the presence of variable external heat flux in the vicinity of the water/silver nanofluid: a molecular dynamics simulation, Case Stud. Therm. Eng. 69 (2025) 105994.
[28] L. Xiao, A. Basem, Y. Zhang, D.J. Jasim, S. Salahshour, Z. Li, D. Toghraie, A numerical study of the effect of variable heat flux on the stability and thermal behavior of SARS-COV-2 structure: a molecular dynamics approach, Case Stud. Therm. Eng. 56 (2024) 104213.
[29] M.R. Smaoui, H. Yahyaoui, Unraveling the stability landscape of mutations in the SARS-CoV-2 receptor-binding domain, Sci. Rep. 11 (1) (2021) 9166.
[30] J. Duplissy, J. Salokas, O. Kivelä, L. Yin, T. Sironen, M. Romantschuk, N.J. A. Atanasova, A field pilot study of the Aero Quattro air purifier operated directly on the air ventilation of a navigating cruise ship: effect on new particle formation and effectiveness against the airborne Phi6 model virus, Aerosol Air Qual. Res. 26 (1) (2026) 4.
[31] X. Zhao, Y. Deng, L. Meng, M. Wang, H. Tian, Y. Wang, C. Zhou, Z. Zhu, H.J. B. Zheng, Cascade signal amplification in hierarchical MOFzymes for revolutionizing electrochemical diagnostics of African swine fever virus, Biosens. Bioelectron. 294 (2026) 118159.
[32] W. Li, H. Gao, M. Cheng, M. Lv, Y. Han, H. Yu, W. Lin, Y. Huang, Z. Lu, Q. Liu, An electrophoretic microfluidic chip for efficient enrichment of broad-spectrum virus at trace-levels, Microchem. J. (2026) 117117.